

# **FRP-Concrete Bond Behavior: A Parametric Study Through Pull-Off Testing**

**by B.M. McSweeney and M.M. Lopez**

**Synopsis:** The sensitivity of the FRP-concrete bond failure load to changes in geometric and material parameters is described, and initial comparisons to predictions from existing bond models are made. To accomplish this, load and strain data from a series of single-lap pull-off tests is analyzed, in which carbon fiber reinforced polymer (CFRP) strips of varying width, thickness, and bonded length were pulled from concrete blocks of varying concrete strength. It was found that the concrete compressive strength had limited effects on the bond failure load, and longer bonded lengths increased the time up to failure load. Changes to the bonded width and FRP thickness had a significant impact on the bond failure load. Failure load predictions produced by three studied bond models were found to be strongly influenced by the material properties used as input, and were occasionally insensitive to the parameters varied.

**Keywords:** bond behavior; bond modeling; CFRP; concrete; fiber-reinforced composite; pull-off test

## 442 McSweeney and Lopez

Brian M. McSweeney graduated with a Master's Degree in Civil Engineering from Penn State University in 2005, and is now a structural engineer at Linton Engineering in Vienna, VA. He earned his B.S. in Civil Engineering from the University of Virginia in 2003. His research is focused on the bond behavior between fiber-reinforced polymer composites and a concrete substrate.

Maria M. Lopez is an Assistant Professor at Penn State University. She is active on several ACI technical committees including committee 544, fiber-reinforced concrete; 543, fracture mechanics; and 440, fiber-reinforced polymer reinforcements. Dr. Lopez's research interests include the use of fiber-reinforced polymer materials for civil infrastructure applications.

### INTRODUCTION

Repair and rehabilitation methods for civil infrastructure in the United States has become a topic of great interest to engineers. In Pennsylvania alone, 40% of the 5,788 concrete bridges are either structurally deficient or functionally obsolete<sup>1</sup>. One relatively new option for the flexural strengthening of concrete members is the use of externally-bonded fiber-reinforced polymer (FRP) laminates. These composite materials consist of an epoxy matrix with fiber reinforcement of either glass, carbon, or aramid materials (GFRP, CFRP, or AFRP, respectively). FRP composites have the benefits of a high strength-to-weight ratio, corrosion resistance, and ease of fabrication. FRP repairs for flexural members can be prefabricated and bonded to the concrete using a separate adhesive, or can be bonded and cured in-situ directly through the epoxy<sup>2</sup> in a process often called wet layup. This study focuses on carbon FRP (CFRP) bonded to concrete using wet layup.

While the use of FRP laminates or sheets bonded to concrete is becoming more common for the repair of concrete flexural members, the behavior of the bond is still in question. The ACI440.2R-02 design guidelines intentionally avoid bond failure between an FRP flexural repair and a concrete substrate as a failure mode. The guidelines incorporate an additional reduction factor into design equations "to arrive at a strain limitation to prevent debonding"<sup>3</sup>. No design equation to calculate bond failure load (given material and geometric properties for the FRP and substrate) has yet been included in these guidelines, but extensive work has been done to propose a number of bond models.

#### **Research Significance**

The objective of this study is to conduct a series of experimental tests to collect data with which three proposed bond models can be evaluated. The study uses the maximum load carried by the bond prior to failure in a pull-off test as an indicator of bond performance, and compares that load to the predicted load from three existing bond models.

## EXPERIMENTAL PROGRAM

To achieve the objective, two sets of (21) 127x127x254mm concrete block specimens were fabricated; one set having an ASTM C39<sup>4</sup> compressive strength ( $f'_c$ ) of 35MPa (Mixture A) and the other set 46MPa (Mixture B). CFRP strips were bonded to the blocks via wet layup after preparing the concrete bonding surfaces by grinding away the laitance. The parameters of interest to this study were the concrete strength, the bonded length of the FRP (76.2, 152.4, and 203.2mm), the bonded width of the FRP (25.4, 50.8, and 76.2mm), and FRP thickness (1, 2, and 3 plies). Table 1 summarizes the parameters and specimens, and Figure 1 illustrates the specimen geometries. Note in Figure 1 that a “narrowing extension” had to be wet-laid with the FRP strip when the bonded width was greater than 25mm so that the strip would fit within the grips, which had a maximum useable width of 25mm. All FRP strips were oriented with the fibers in the longitudinal direction ( $0^\circ$ ).

A restraint frame was designed and constructed for the 49kN load frame used during testing, as shown in the sketch in Figure 2. Placing a plate (the “crack shim”) between the top of the concrete block and the top plate of the restraint with a 25mm setback created a free edge for the concrete. The effects of this free edge were studied during testing.

Three specimens were tested for each parameter of interest, as indicated in Table 1. Out of each set of three, one specimen was instrumented with 120 $\Omega$  strain gages at the center of the bonded width. Load-displacement data was collected for all specimens, and strain data was available for each parametric variation. Although the maximum load transferred by the FRP-concrete bond was the key factor in the comparison to existing bond models, the strain data aided in evaluating the bond behavior. Figure 3 depicts the strain gage layout on the specimens.

## TESTING AND OBSERVATIONS

Each specimen was carefully secured in the restraint frame and checked for alignment with the grips to prevent normal stresses from forming along the bonded length. Normal (peeling) stresses have been shown to have a significant effect on the bond behavior<sup>5</sup>. Sandpaper was placed between the self-tightening grips and the CFRP strips to ensure that slip would not occur.

Testing was conducted on the specimens under a displacement-controlled rate of 0.381mm per minute. Using this rate, the specimens reached failure within 7 to 15 minutes on average, and the propagation of the crack front through the CFRP-concrete bond was found to be stable. Data was collected at 20 points / second (20Hz). When an instrumented specimen was tested, the gages were connected to a ¼ Wheatstone bridge to collect strain data.

## 444 McSweeney and Lopez

### Propagation of Failure Through the Bond

During the initial portion of the test procedure (the first few minutes), the specimens did not display any signs of distress. After a few minutes, cracking and small popping sounds could be heard as the load applied to the strip (and the bond) continued to increase. Near the end of each test, as the final bond failure approached, cracking sounds became louder and occurred at much shorter intervals. On occasion, just prior to complete failure, the cracking came in a continuous string, analogous to an unzipping sound. This has been observed in other tests, such as those conducted by Lopez in 2000<sup>6</sup>.

As bond failure progressed, small diagonal cracks began to form in the edges of the CFRP strips, as shown in Figure 4. These cracks appeared at regular intervals, and never propagated significantly inwards from the edges of the strip. The angle of the cracks suggests an edge effect, affecting the crack front propagation, seen clearly in the crack front of a GFRP strip bonded to steel in Figure 4, tested by the author prior to this study. Each new crack in the CFRP strips appeared at a time approximately corresponding to a shift in the crack front as a portion of the FRP-substrate bond fails.

As tests progressed, 86% of the 42 specimens developed cracks in the concrete substrate that ran from the edge of the FRP strip up to a point at the leading edge of the concrete block. Figure 5 depicts these cracks, which resulted in a tooth of concrete at the top of the block. The angle,  $\alpha$ , tended to increase as the bonded width of the strip increased, but the distance,  $x$ , remained the same, leading to a wider tooth of concrete at the free edge. Rarely did the tooth approach the edge of the shim plate used in the restraint setup – thus, the unrestrained edge distance of 25mm between the shim plate and the bonding surface was sufficient to prevent an unrealistic restraint of the concrete against failure. The tooth did not displace visibly during testing, but upon final bond failure, the tooth remained bonded to the FRP strip. Concrete cover failure as part of overall bond failure has been noted by several researchers, including Lopez in 2003<sup>7</sup> and Buyukozturk in 1998<sup>8</sup>.

### Final Bond Failure

The final failure of the CFRP-concrete bond was extremely brittle, and accompanied by a large release of energy. Some of the FRP strips were damaged by the energy release at final failure, exhibiting splitting in the longitudinal (fiber) direction, while the epoxy of some other strips had transverse cracking post failure. Fragments of concrete were torn from the block when the strip broke free.

Increased bonded length, width, and thickness parameters led to longer time-to-failure, but changes to the bonded width had the greatest impact on time-to-failure. For the shortest bonded length (76mm), there was little warning before final failure. All other FRP strips provided some warning, prior to final bond failure, in the form of the cracking sounds.

While a few specimens experienced pull-out of an additional tooth of concrete at the end of the bonded length during failure, the vast majority only lost the concrete tooth at the leading edge of the bond as discussed previously. The remainder of the bonded

region past the leading edge on the concrete block was free of epoxy after failure, and the FRP strips did not exhibit a significant amount of paste left clinging to the strip. However, the concrete surface was rough, with numerous microcracks oriented in a manner indicative of the direction of bond failure progression. A pattern of regularly-spaced microcracks was visible throughout the bonded area, with small pieces of paste peeled back by the propagation of the bond failure as shown in Figure 6.

## EXPERIMENTAL RESULTS

The data obtained from experimentation can be subdivided into three categories. These are the maximum load data, which was compared to failure load predictions from existing bond models; load-displacement data; and strain data along the bonded region. The “base specimen” for comparison is defined as a block with a 1-ply FRP strip, a 25mm bonded width, and a 152mm bonded length. The average failure load for this specimen is defined as  $P^*$ .

### Maximum Load Data

Results for the maximum load carried by the CFRP-concrete bond ( $P_{max}$ ) are summarized in Figures 7(a) and (b). The data had relatively little scatter, with an average coefficient of variance (CV) of 7.83%. The limited scatter is a strong indication of the validity of the data presented in this report.

From these figures and the values obtained for  $P_{max}$ , it can be seen that concrete strength did not have a significant impact on the maximum load carried by the bond for this type of test. Maximum loads either increased slightly by about 1% or decreased slightly by around 7% – this variation can be associated with differences in specimen fabrication or inherent material variability in the concrete.

Figures 8(a) and (b) show the changes in the normalized failure load ratio ( $P_{max} / P^*$ ) as the parameters of study change. The  $P_{max}$  value used here for the comparisons is the average from each group of three specimens from both Mixture A and B. When the bonded length changed from 76mm to 152mm, the failure load ratio increased by about 17%; beyond 152mm bonded length, the failure load did not increase significantly, and in fact decreased by about 4%. This behavior is believed to be related to the fact that the bonded length may have exceeded the effective bonded length as defined by Täljsten<sup>9</sup> after 152mm. Thus, the additional bonded length only increased the time to failure for the system. This, then, indicates that an increase in bonded length beyond the length needed to transfer stresses between the FRP and concrete can provide some warning time prior to the FRP-concrete system failure. However, the extra length will not significantly impact the system failure load.

On average, increasing the bonded width had more impact on the bond failure load (an increase of approximately 95% from 25mm bonded width to 76mm bonded width) than an increase in the FRP thickness (which caused a total failure load increase of approximately 55% from 1 to 3 plies). Increasing bonded width, while shown here to be effective at adding to the load capacity of the FRP-concrete system, may not be practical

## 446 McSweeney and Lopez

due to limitations imposed by the width of the member being repaired. Extra plies of FRP added to the load capacity of the system as well, so when increasing bonded width is not an option, adding to the repair thickness will still increase the failure load substantially.

The relationship between changes in each parameter and the resulting failure load increase was investigated. It was found that the failure loads did not increase by the same ratio as the FRP thickness or width – that is to say, the failure load did not double when the bonded width or FRP thickness doubles. Moreover, the incremental changes in failure load for changes in each parameter were not necessarily linear for the data obtained in this study, as seen for the FRP thickness. The increase in the ratio of Figures 8(a) and (b) from one to two plies was approximately 25%, while the increase in the ratio from two to three plies was 31%. However, the change was linear for additional bonded width, with an increase of 48% from 25mm to 51mm of bonded width and 47% from 51mm to 76mm of bonded width. More testing may need to be done to determine if the nonlinearity for the changes in FRP thickness is due to inherent variability in the data. Because the load-carrying capacity of the system does not increase in a one-to-one manner for added width or quantity of plies, it may be necessary to vary multiple parameters at once when designing an FRP flexural strengthening solution to obtain the desired amount of additional load capacity for the system.

### Strain Data

The strain data collected supports observations by researchers such as Täljsten<sup>9</sup> and Miller and Nanni<sup>10</sup>. Figures 9, 10 and 11 for the Mixture A specimens, respectively, show that as the load was initially applied to the specimens, the strains on the FRP near the free edge of the concrete increased steadily until bond failure began. At that point, if strain redistribution was able to occur along the bonded length (i.e., additional bonded length was available for crack propagation to occur prior to bond failure), the strain near the free edge of the bonded length reached a peak value and remained near that value for the remainder of the test. Meanwhile, strain began to increase at the next gage on the bonded length, and so forth as the crack propagated until complete debonding failure occurred. Debonding failure is believed to result from a condition where the remaining bonded length is insufficient to transfer stresses between the FRP and the concrete substrate.

Specimens with longer bonded length, greater width, and greater thickness experienced this strain redistribution at higher loads. Also, strains in specimens with greater thickness or bonded width tended to be smaller in magnitude than the strains in the specimens with one ply of carbon fiber and 25mm of bonded width for the same load. Longer bonded length did not reduce the magnitude of strain at the location of the strain gages, but it did ensure that strain redistribution could occur (again, increasing the time up to failure of the system). For the 76mm bonded length, strain redistribution did not occur to any significant degree prior to complete bond failure.

Plots for the Mixture B specimen strain data were similar in nature to those presented for Mixture A. As with the load data, the difference in concrete compressive strength between Mixtures A and B had little impact on the strain data.

### **Load-Displacement Data**

Additional information about the bond behavior can be obtained from the crosshead load and displacement data. Figure 12 illustrates the load-displacement relationships for the specimens of Mixture A.

After an initial adjustment period, and prior to the beginning of debonding, the slopes of the load-displacement curves exhibited similar slopes for each set of three specimens. For those specimens with varied bonded length, the slopes of all specimens matched quite well for each mixture (A and B). However, as bonded width and FRP thickness increase, the slopes increase. This indicates that while an increase in bonded length for the FRP strip does not change the overall stiffness of the FRP-concrete system, an increase in bonded width or FRP thickness can strongly influence the stiffness of the system. Future research should consider other types of FRP material (such as GFRP) bonded to concrete and examine the changes in stiffness for that system as the same parameters are varied. Specimens with a greater bonded width or FRP thickness experience less deformation for a given load. Increasing the bonded length from 76mm to 152mm increases the displacement of the FRP-concrete system in proportion to the increase in maximum load. However, as also seen in the maximum load data, an increase from 152mm to 203mm of bonded length results in little change in maximum load and displacement values.

At the higher bonded lengths, it can be noted that the load-displacement curve appears to reach a plateau where the load continues to increase and drop repeatedly within a narrow range of load values, until complete bond failure. This supports the concept of an effective or active strain transfer region<sup>9</sup> that shifts as the bond failure propagates. When the effective strain transfer region reaches its maximum capacity for strain transfer, bond failure occurs in that region, forcing the region to shift down the bonded length. The load drops momentarily, reducing the strains; then, the strains increase again in the new transfer region until they reach the maximum capacity once again, and so forth.

### **Edge Effects**

By examining the load-displacement and normalized failure load ratio ( $P_{max} / P^*$ ) data for those specimens with bonded width variant, it can be seen that the aforementioned edge effects may influence system failure load results for specimens less than 51mm in bonded width. The increase in the normalized failure load ratio is greater between 25mm and 51mm than between 51mm and 76mm for both Mixture A and B. Similarly, the change in crosshead displacement at failure is greater between 25mm and 51mm of bonded width than between 51mm and 76mm. This data, in conjunction with the observed crack patterns, supports the theory that the bond behavior for narrow FRP strips is influenced by the U-shaped crack front – the apparent FRP-concrete system capacity may be less than expected. For wider strips, the influence of these edge effects

## 448 McSweeney and Lopez

becomes negligible relative to the overall width of the strip. Further study is required to confirm this, as it has significant implications for the validity of results obtained in previous studies by other researchers, which often used strips 25mm in width.

### ANALYTICAL STUDY

The experimental results are compared to maximum load predictions from three existing bond models, as proposed by Maeda et al. in 1997<sup>11</sup> (Model 1), Miller and Nanni in 1999<sup>10</sup> (Model 2), and Chen and Teng in 2001<sup>12</sup> (Model 3). These three models were chosen because the models incorporate equations to find effective bond length and also to find the maximum load the FRP-concrete system can carry. Model 2 is a variation on Model 1.

The input to these models includes the actual material properties obtained during the course of experimentation and through coupon testing, as well as published material properties for the CFRP system. Table 2 summarizes the necessary input values for each model.

Two different modulus of elasticity values were used for the FRP as input. The first modulus, called the *nominal* modulus of elasticity (*Nom. E*), is based upon the manufacturer's published fiber modulus. This is used in conjunction with the published FRP thickness (again, based upon the fiber cloth thickness) and the other input values to generate the nominal modulus line on each plot of failure load output. The second modulus, called the *actual* modulus (*Act. E*), is based on coupon testing data of CFRP strips. This is used in conjunction with the actual measured specimen thickness values and the other input values to generate the actual modulus line.

The failure load output for the models is plotted as a continuous curve over the range for each parameter studied, with the experimental data shown on the same plot. This output is shown in Figures 13, 14, and 15 for Mixture A.

The plots in Figure 13 show that Models 1 and 2 are insensitive to changes in the bonded length, while Model 3 follows the trend of the data but is too conservative for longer bonded lengths. Models 1 and 2 do not predict the decrease in failure load for the FRP-concrete system as bonded length becomes shorter than 152mm, but remain conservative within the data range of 76 – 203mm bonded length when the nominal manufacturer's values for  $E_{FRP}$  and FRP thickness are used.

From the plots in Figure 14, it can be seen more clearly that the models were calibrated using published (nominal) values for  $E_{FRP}$  and FRP thickness, as these values give better predictions of the failure loads. All three models follow the trend in the  $P_{max}$  values; Models 1 and 2 result in a linear trend, and Model 3 in a power curve trend. Model 2 has a steeper slope than Model 1, and may overestimate the failure load for the FRP-concrete system at higher values of bonded width.

The plots of Figure 15 indicate that all models predict changes in the failure load for increasing FRP thickness with changes in slope as plies are added. The failure load predictions from Model 2 best correlate to the shape of the trend in the data for increasing FRP thickness. It is conservative with respect to the data by a consistent amount. The other two models seem to predict a greater change in failure load from two to three plies than from one to two plies – this does not match the trends in the experimental data. Moreover, all three models are conservative with respect to the failure loads. Since adding layers of FRP is one of the primary methods used to obtain extra capacity in externally-bonded FRP repairs, this particular lack of sensitivity to trends in the data will require further study and analysis. As with Figure 14, these plots indicate that using the actual composite properties as input (as opposed to nominal properties) has a negative impact on the failure load predictions for these three particular models, rendering them completely insensitive to thickness changes.

Output for Mixture B was quite similar to the output for Mixture A both in trends and magnitudes of  $P_{max}$  for variations in the parameters of interest.

## CONCLUSIONS AND RECOMMENDATIONS

This study has created a new database of experimental data for modeling the bond behavior of the FRP-concrete system.

### Conclusions

The failure load of the FRP-concrete system depends primarily upon the width of the bonded region and the thickness of the FRP repair. Increasing the bonded width had the greatest effect on increasing the failure load of the system, but may be limited by the geometry of the member being repaired. Increases in FRP thickness also significantly increased the failure load of the system.

Bond failure occurs in stages, provided there is sufficient bonded length to develop the full capacity of the bond in more than one region. The strain data and load-displacement data both support this observation.

Failure of the bond at a free edge, such as at a crack in a beam, will most likely result in the pull-out of a tooth of concrete before the bond begins to fail at the epoxy-concrete interface. Final catastrophic failure of the FRP-concrete bond is extremely brittle. The energy release is sufficient to also fail the FRP itself in some cases, and to tear out teeth of concrete.

Edge effects were observed during testing that may influence the results obtained using specimens with FRP strips less than 51mm in bonded width, which may have negatively impacted results obtained in previous studies of the FRP-concrete bond.

All of the studied bond models appear to be calibrated to nominal material properties (modulus of elasticity and thickness of the FRP). If actual composite

## 450 McSweeney and Lopez

properties obtained from material testing are used, the models may not be conservative in the predictions of failure load.

The models from Maeda et al.<sup>11</sup> and Miller and Nanni<sup>10</sup> are both insensitive to changes in failure load as bonded length changes. While this is acceptable when the bonded length exceeds the effective bonded length, it may be unconservative for bonded lengths shorter than the effective length.

All three models are relatively accurate in their predictions for failure loads as bonded width varies. Miller and Nanni's<sup>10</sup> model may over-predict the failure load for bonded widths greater than those studied despite having the closest correlation to the failure loads in the range of the data gathered.

The models studied underestimate the performance gain from increased FRP thickness. The model developed by Miller and Nanni<sup>10</sup> shows a closer trend to the experimental failure loads with increasing FRP thickness.

Overall, Miller and Nanni's model<sup>10</sup> fit the data more closely than the other two. However, the trends in the experimental data are most accurately modeled by Chen and Teng's bond model<sup>12</sup>.

### **Recommendations**

Results from this study show that further study must be devoted to developing and extensively testing a unified bond model for external FRP reinforcement bonded to concrete. While it is believed that other FRP materials (such as glass FRP) bonded to concrete may exhibit similar results, testing should be done on such systems to determine the influence of the change in FRP elastic modulus on the test results, as compared to the CFRP results presented here. Once a complete bond model for FRP-concrete systems is developed and tested, it can be integrated into the ACI 440 design guidelines.

### **ACKNOWLEDGEMENT**

The author thanks the National Science Foundation for its support of the research activity described in this study (grant CMS 0330592).

### **REFERENCES**

- [1] Federal Highway Administration, "Material Type of Structure by State" Bridge Technology (2004), Excel File, <http://www.fhwa.dot.gov/bridge/mat03.xls> (accessed February 25, 2004).
- [2] Bakis, C.E., et al., "Fiber-Reinforced Polymer Composites for Construction – State-of-the-Art Review." *Journal of Composites for Construction*, V6 (2002), pp. 73-87.
- [3] American Concrete Institute. ACI440.2R-02: Guide for the Design and Construction of Externally Bonded FRP Systems for Strengthening Concrete Structures. Farmington Hills, MI, ACI, 2002.

- [4] American Society for Testing of Materials. "ASTM C39 / C39 M: Standard Test Method for Compressive Strength of Cylindrical Concrete Specimens." Annual Book of ASTM Standards. Conshohocken: ASTM, 2001.
- [5] Karbhari, V.M., et. al. "On the Durability of Composite Rehabilitation Schemes for Concrete: Use of a Peel Test." *Journal of Materials Science* 32 (1997), pp. 147 - 156.
- [6] Lopez, M.M. "Study of the Flexural Behavior of Reinforced Concrete Beams Strengthened by Externally Bonded Fiber Reinforced Polymeric (FRP) Laminates." Ph.D. Thesis University of Michigan, 2000.
- [7] Lopez, M.M., and A.E. Naaman. "Concrete Cover Failure or Tooth Type Failure in RC Beams Strengthened with FRP Laminates." *Fiber-Reinforced Polymer Reinforcement for Concrete Structures, Proc. of the Sixth International Symposium on FRP Reinforcement for Concrete Structures*, 8-19 Jul. 2003, Singapore. Ed. Kiang Hwee Tan. River Edge: World Scientific Publishing Co., 2003., pp. 317 - 326.
- [8] Buyukozturk, Oral, and Brian Hearing. "Failure Behavior of Precracked Concrete Beams Retrofitted with FRP." *Journal of Composites for Construction* 2 (1998): pp. 138-144.
- [9] Täljsten, Björn. "Defining Anchor Lengths of Steel and CFRP Plates Bonded to Concrete." *Journal of Adhesion and Adhesives Great Britain: Elsevier Sci. Ltd*, 1998.
- [10] Miller, Brian, and Antonio Nanni. "Bond Between CFRP Sheets and Concrete." *Proc., ASCE 5<sup>th</sup> Materials Congress*, 10-12 May 1999, Cincinnati. Ed. L.C. Bank, pp. 240-247.
- [11] Maeda, Toshiya, et al. "A Study on Bond Mechanism of Carbon Fiber Sheet." *Non-Metallic (FRP) Reinforcement for Concrete Structures. Proc. of the Third International Symposium*, Vol. 1, Oct. 1997, Japan: Japan Concrete Institute, pp. 279-286.
- [12] Chen, J.F., and J.G. Teng. "Anchorage Strength Models for FRP and Steel Plates Bonded to Concrete." *Journal of Structural Engineering* 127 (2001), pp. 784-791.

# 452 McSweeney and Lopez

Table 1 – Test Matrix

		Mixture A					
		Varying $b_{FRP}$			Varying $L_b$		Varying $t_{FRP}$
Specimen No.		1,2,3	4,5,6	7,8,9	10,11,12	13,14,15	16,17,18 19,20,21
Plate Thickness (# of plies)		1	1	1	1	1	2 3
Bonded Length (mm)		152	152	152	76	203	152 152
Bonded Width (mm)		25	51	76	25	25	25 25
		Mixture B					
Specimen No.		22,23,24	25,26,27	28,29,30	31,32,33	34,35,36	37,38,39 40,41,42
Plate Thickness (# of plies)		1	1	1	1	1	2 3
Bonded Length (mm)		152	152	152	76	203	152 152
Bonded Width (mm)		25	51	76	25	25	25 25

Table 2 – Input values needed for each model

Model	Concrete Width	$f_c$	FRP Thickness	Bonded Width	Bonded Length	$E_{FRP}$ (Elastic Modulus)	Strain Gradient ( <i>constant</i> )
1			X	X	X	X	X
2			X	X	X	X	X
3	X	X	X	X	X	X	

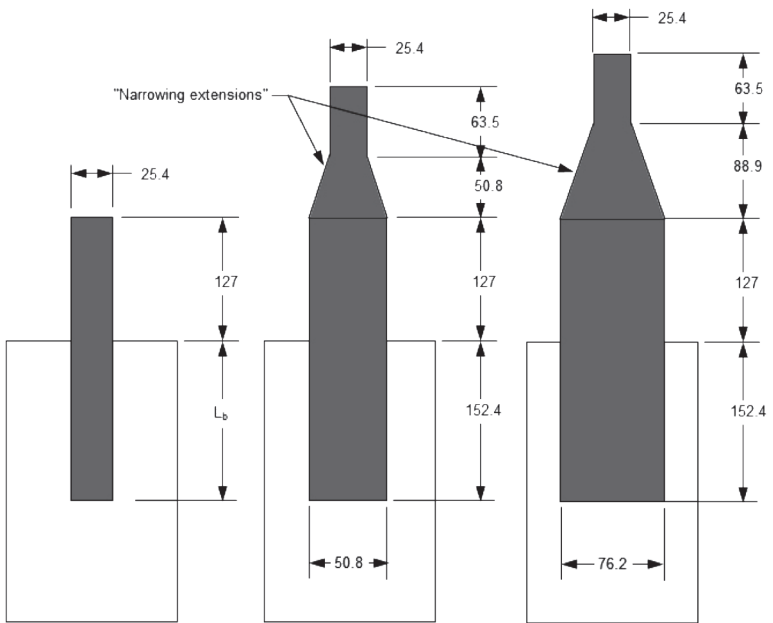


Figure 1 – Sketch of specimen geometries (not to scale)

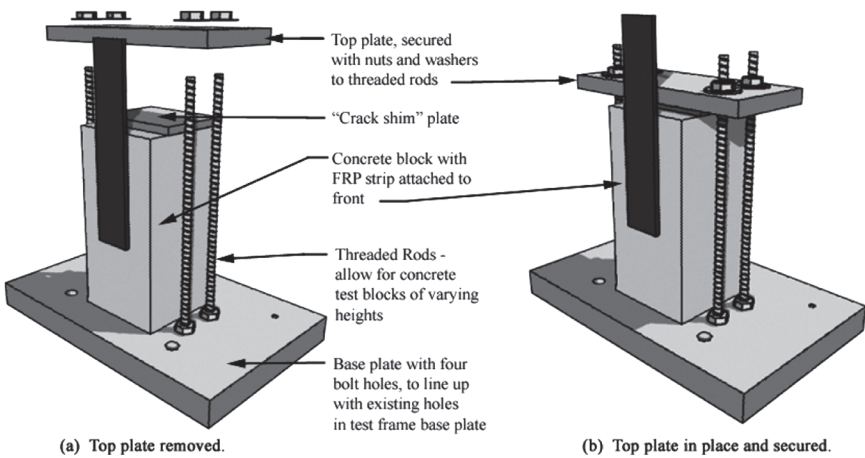


Figure 2 – Sketch of the restraint frame for specimens

# 454 McSweeney and Lopez

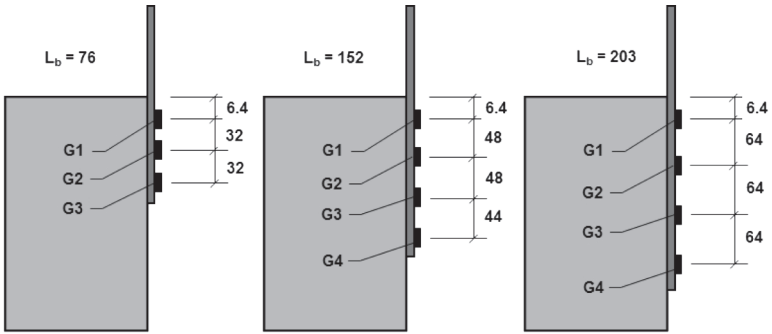


Figure 3 – Sketch of specimen instrumentation along the bonded length (not to scale).

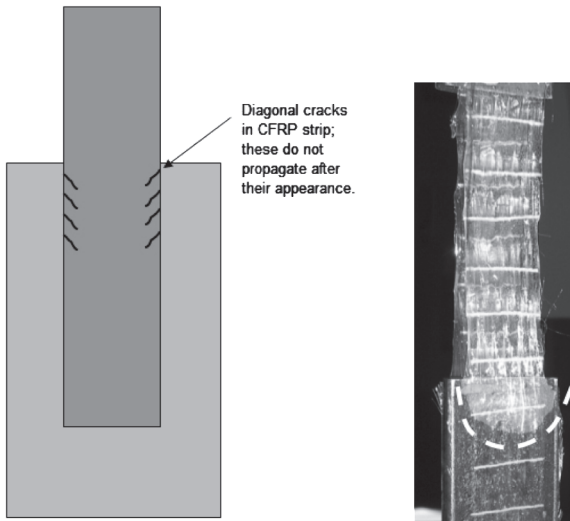


Figure 4 – Exaggerated sketch of edge cracking in the CFRP during testing, compared to edge effects observed in GFRP strips bonded to steel.

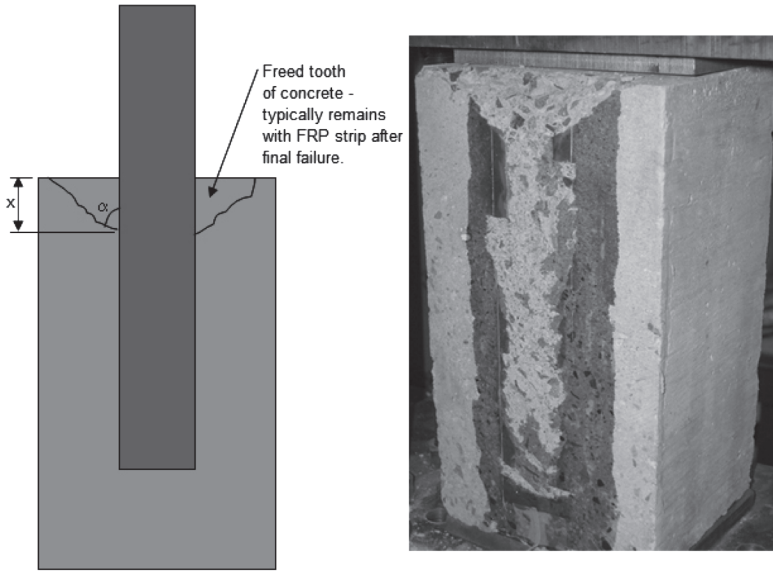


Figure 5 – Free edge failure of the concrete.

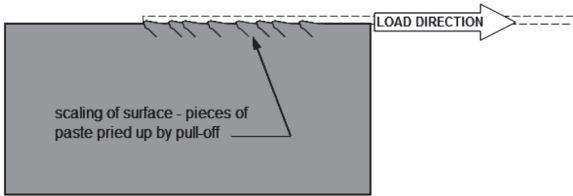


Figure 6 – Concrete surface scaling due to pull-off of the FRP strip.

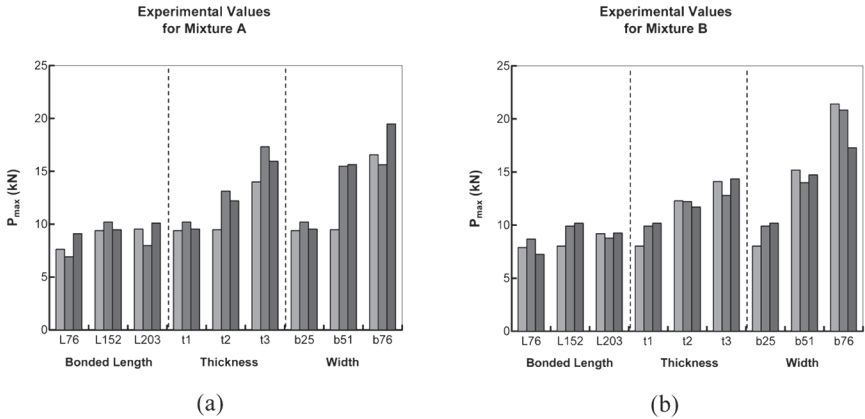
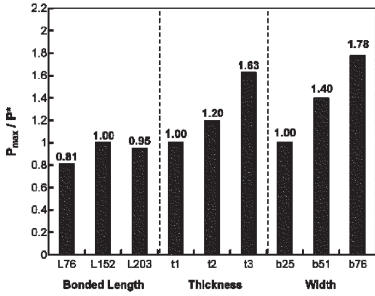


Figure 7 – (a)  $P_{max}$  - results for Mixture A (b)  $P_{max}$  results for Mixture B.

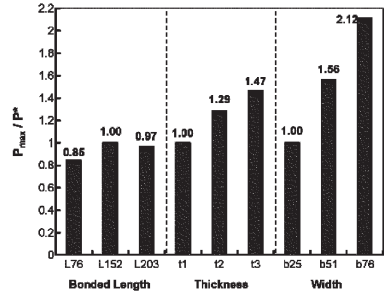
# 456 McSweeney and Lopez

Failure Load Comparisons Relative to "Base Specimen"  
Failure Load,  $P^*$ : Mixture A



(a)

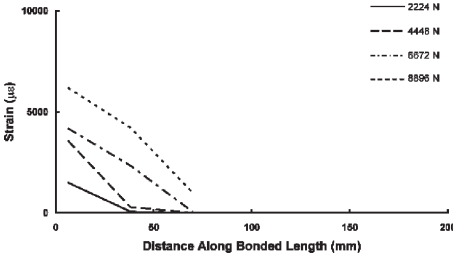
Failure Load Comparisons Relative to "Base Specimen"  
Failure Load,  $P^*$ : Mixture B



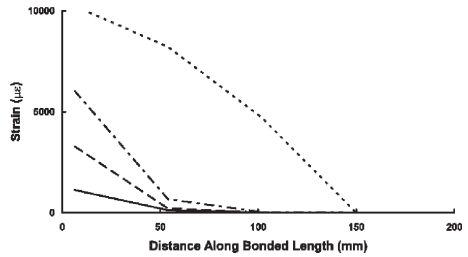
(b)

Figure 8 – (a)  $P_{max} / P^*$  for Mixture A (b)  $P_{max} / P^*$  for Mixture B.

Strain Behavior for 76mm Bonded Length



Strain Behavior for 152mm Bonded Length



Strain Behavior for 203mm Bonded Length

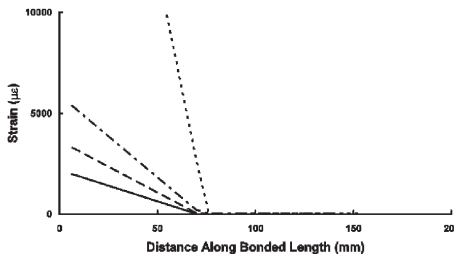


Figure 9 – Strain data as bonded length varies: Mixture A specimens.

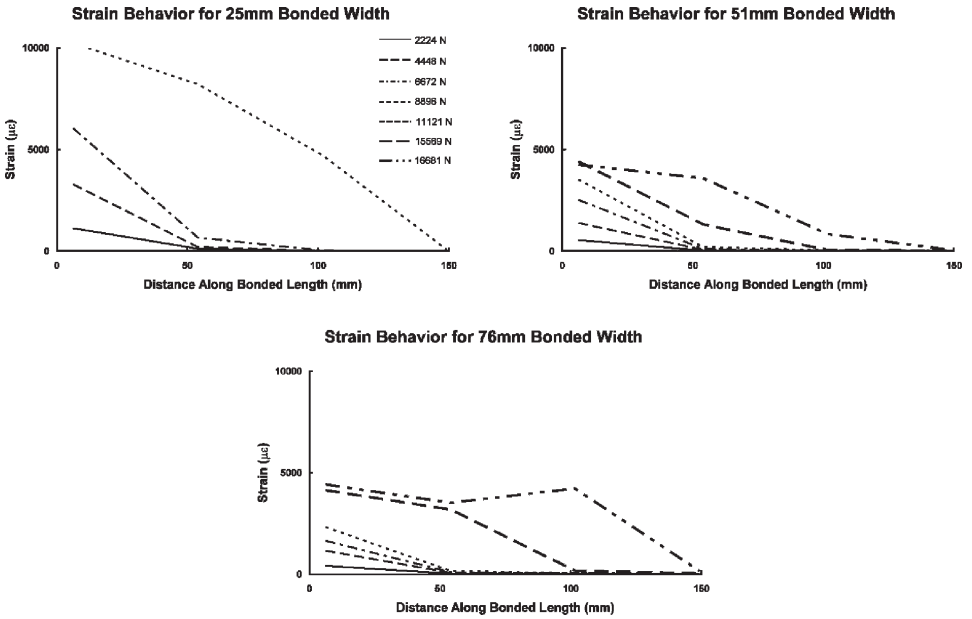


Figure 10 – Strain data as bonded width varies: Mixture A specimens.

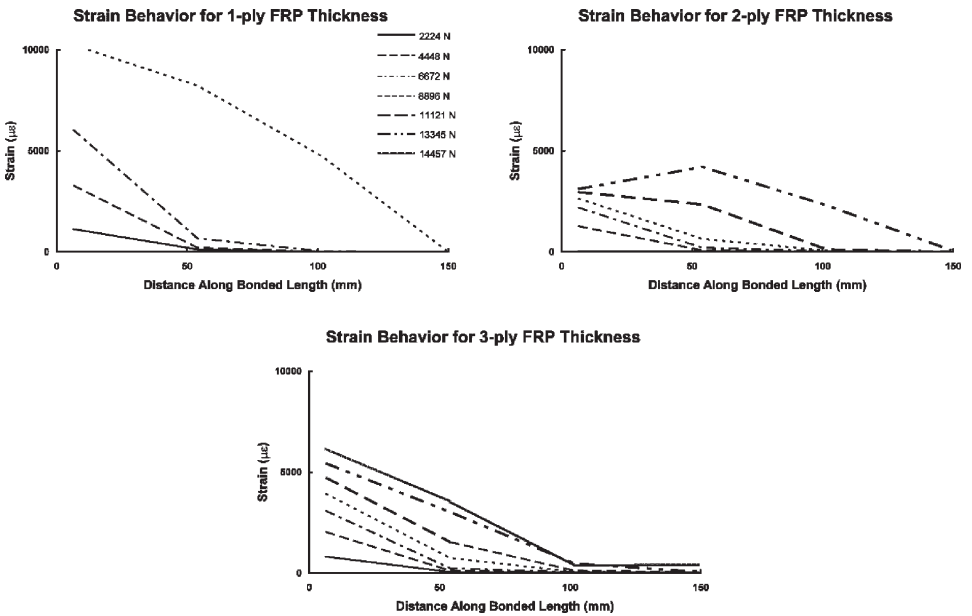
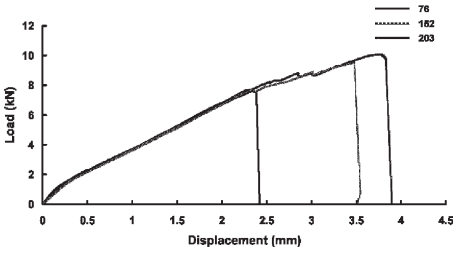


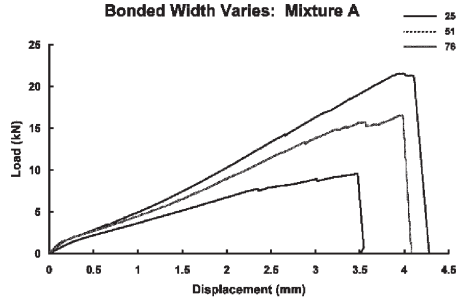
Figure 11 – Strain data as FRP thickness (number of plies) varies: Mixture A specimens.

# 458 McSweeney and Lopez

Bonded Length Varies: Mixture A



Bonded Width Varies: Mixture A



Load-Displacement Behavior for Varied FRP Thickness: Mixture A

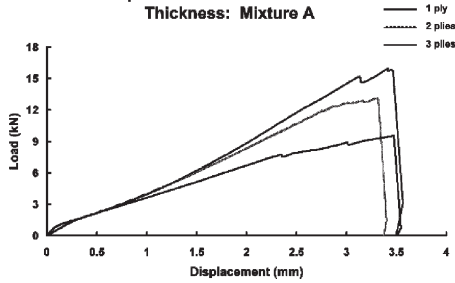
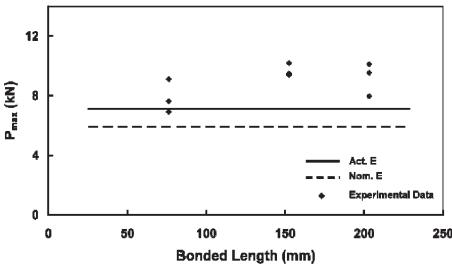
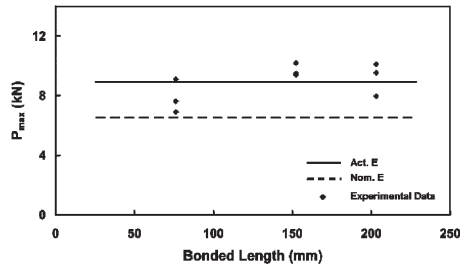


Figure 12 – Typical load-displacement results for the parameters studied: Mixture A.

Model 1: Bonded Length Varies  
Mixture A



Model 2: Bonded Length Varies  
Mixture A



Model 3: Bonded Length Varies  
Mixture A

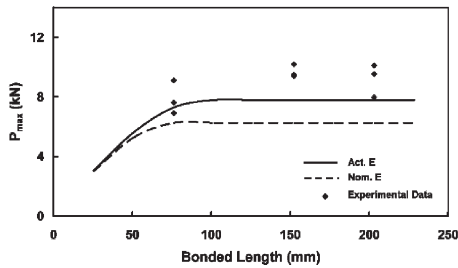


Figure 13 – Model predictions for bonded length variant: Mixture A.

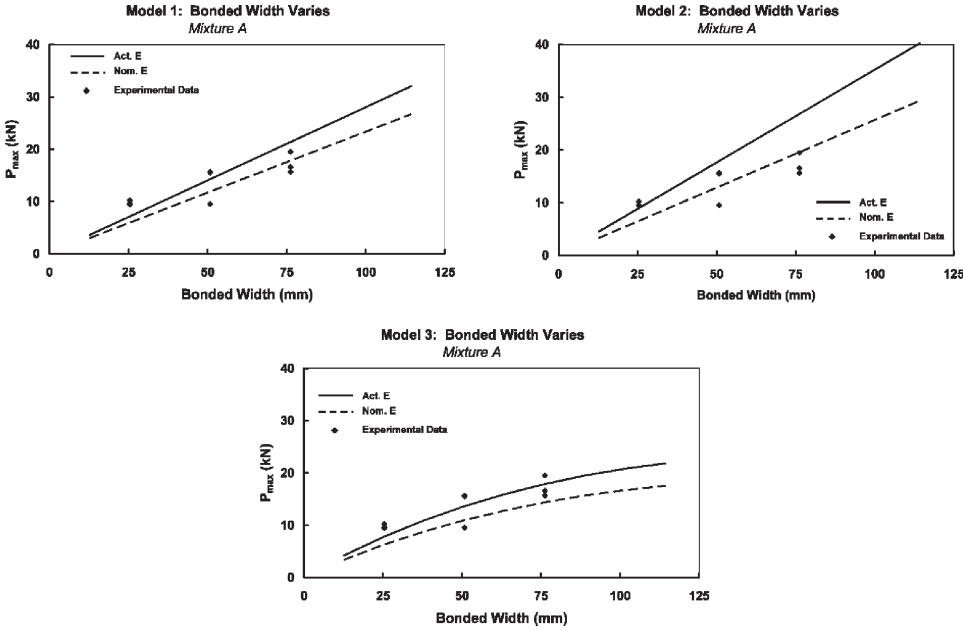


Figure 14 – Model predictions for bonded width variant: Mixture A.

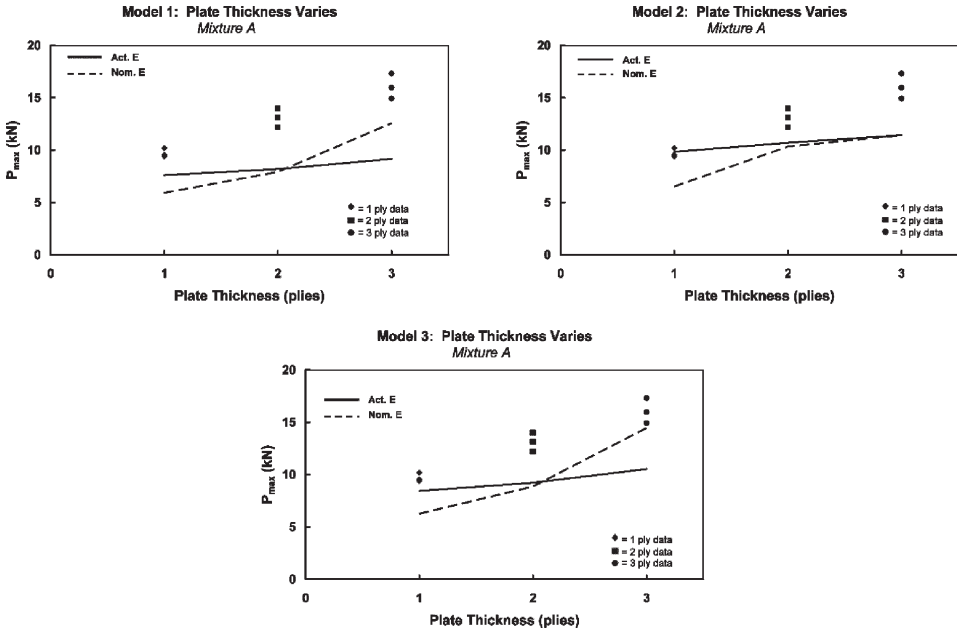


Figure 15 – Model predictions for FRP thickness (plies) variant: Mixture A.

